ORIGINAL ARTICLE

Diagnostic accuracy of ^{68}Ga-DOTANOC PET/CT imaging in pheochromocytoma

Punit Sharma · Varun Singh Dhull · Saurabh Arora · Poonam Gupta · Rajeev Kumar · Prashant Durgapal · Arun Malhotra · Sunil Chumber · Ariachery C. Ammini · Rakesh Kumar · Chandrasekhar Bal

Abstract

Purpose The purpose of the present study was to evaluate the diagnostic accuracy of ^{68}Ga-DOTANOC positron emission tomography (PET)/CT in patients with suspicion of pheochromocytoma.

Methods Data of 62 patients [age 34.3 ± 16.1 years, 14 with multiple endocrine neoplasia type 2 (MEN2)] with clinical/biochemical suspicion of pheochromocytoma and suspicious adrenal lesion on contrast CT ($n=70$), who had undergone ^{68}Ga-DOTANOC PET/CT, were retrospectively analyzed. PET/CT images were analyzed visually as well as semiquantitatively, with measurement of maximum standardized uptake value (SUV_{max}), SUV_{mean}, SUV_{max}/SUV_{liver}, and SUV_{mean}/SUV_{liver}. Results of PET/CT were compared with ^{131}I-metaiodobenzylguanidine (MIBG) imaging, which was available in 40 patients (45 lesions). Histopathology and/or imaging/clinical/biochemical follow-up (minimum 6 months) was used as reference standard.

Results The sensitivity, specificity, and accuracy of ^{68}Ga-DOTANOC PET/CT was 90.4, 85, and 88.7 %, respectively, on patient-based analysis and 92, 85, and 90 %, respectively, on lesion-based analysis. ^{68}Ga-DOTANOC PET/CT showed 100 % accuracy in patients with MEN2 syndrome and malignant pheochromocytoma. On direct comparison, lesion-based accuracy of ^{68}Ga-DOTANOC PET/CT for pheochromocytoma was significantly higher than ^{131}I-MIBG imaging (91.1 vs 66.6 %, $p=0.035$). SUV_{max} was higher for pheochromocytomas than other adrenal lesions ($p=0.005$), MEN2-associated vs sporadic pheochromocytoma ($p=0.012$), but no difference was seen between benign vs malignant pheochromocytoma ($p=0.269$).

Conclusion ^{68}Ga-DOTANOC PET/CT shows high diagnostic accuracy in patients with suspicion of pheochromocytoma and is superior to ^{131}I-MIBG imaging for this purpose. Best results of ^{68}Ga-DOTANOC PET/CT are seen in patients with MEN2-associated and malignant pheochromocytoma.

Keywords Pheochromocytoma · ^{68}Ga-DOTANOC · PET/CT · MIBG

P. Sharma · V. S. Dhull · S. Arora · R. Kumar · A. Malhotra · R. Kumar · C. Bal (✉)
Department of Nuclear Medicine, All India Institute of Medical Sciences, Ansari Nagar, New Delhi 110029, India
e-mail: csbal@hotmail.com

P. Gupta · A. C. Ammini
Department of Endocrinology and Metabolism, All India Institute of Medical Sciences, New Delhi, India

P. Durgapal
Department of Pathology, All India Institute of Medical Sciences, New Delhi, India

S. Chumber
Department of Surgical Disciplines, All India Institute of Medical Sciences, New Delhi, India

Introduction

Pheochromocytomas are rare tumors arising from the chromaffin cells of the adrenal medulla [1]. They represent a rare (<1 %) but potentially curable cause of hypertension [2]. While the majority of pheochromocytomas are sporadic, in about a quarter of unselected cases they may be associated with hereditary syndromes like multiple endocrine neoplasia (MEN), von Hippel-Lindau syndrome (VHL), neurofibromatosis 1, and tuberous sclerosis [3]. The diagnosis of pheochromocytoma is established by measurement of

blood and urinary catecholamines or their metabolites, followed by demonstration of an adrenal mass on anatomical (CT/MRI) imaging. However, biochemical markers have high sensitivity (96–100 %), but low specificity (69 %) for the detection of pheochromocytomas [4]. Similarly, the specificity of CT or MRI is also limited for differentiating pheochromocytoma from other adrenal lesions [5]. These limitations have led to reliance on functional imaging methods in order to avoid unnecessary surgery.

$^{131/123}$I-Metaiodobenzylguanidine (MIBG) scintigraphy is currently the functional imaging of choice for pheochromocytoma [6], but suffers from drawbacks like limited spatial resolution, difficulty in detection of small tumors (<1.5–2.0 cm), or large tumors with extensive necrosis/hemorrhage, lack of tracer uptake in some tumors, and interference with certain medications, all of which can lead to false-negative results [7]. Addition of single photon emission computed tomography (SPECT) improves the sensitivity [8], but even then the spatial resolution is low (~1.5 cm) and the detection of small lesions is often difficult. Given the superior resolution of positron emission tomography (PET) over SPECT, functional imaging of pheochromocytoma has been attempted with a wide array of PET tracers like ^{18}F-fluorodeoxyglucose (FDG) [9], ^{18}F-fluorodopa (FDOPA) [10], ^{18}F-fluorodopamine (FDA) [11], ^{11}C-hydroxyephedrine (HED) [12], and ^{68}Ga-DOTA-peptides [13] with encouraging results. Expression of somatostatin receptors (SSTR) by pheochromocytomas [14] facilitates targeted PET imaging with ^{68}Ga-DOTA-peptides (^{68}Ga-DOTATOC, ^{68}Ga-DOTANOC, and ^{68}Ga-DOTATATE). However, to date very few studies have evaluated ^{68}Ga-DOTA-peptide PET/CT (only one with ^{68}Ga-DOTANOC) in pheochromocytomas and only in small and mixed patient populations [15–19]. Therefore, the purpose of the present study was to comprehensively evaluate the diagnostic accuracy of ^{68}Ga-DOTANOC PET/CT in a large number of patients with suspected pheochromocytoma and compare the results with ^{131}I-MIBG imaging when available (^{123}I-MIBG is not available in our country).

Materials and methods

The present retrospective study was approved by the Institutional Ethics Committee and because of the retrospective nature written informed consent was waived. The inclusion criteria were clinical and/or biochemical suspicion of pheochromocytoma along with adrenal abnormality on contrast CT. The biochemical suspicion was based on the presence of one or more of the following: urinary epinephrine (>20 μg/day), urinary norepinephrine (>90 μg/day), urinary vanillylmandelic acid (>7.9 mg/day), urinary total metanephrine (>1.2 mg/day), plasma epinephrine (>85 pg/ml), plasma norepinephrine (500 pg/ml), plasma metanephrine (>400 pg/ml), plasma normetanephrine (>676 pg/ml), and plasma methoxytyramine (>1,800 pg/ml). A total of 62 patients who underwent ^{68}Ga-DOTANOC PET/CT between March 2007 and December 2012 satisfied the inclusion criteria. Data of these 62 patients were retrieved from departmental registries and analyzed. In addition, 40 of these 62 patients also had undergone ^{131}I-MIBG scintigraphy. Of these 62 patients, 10 had been previously included in the pilot study by Naswa et al. [18].

^{68}Ga-DOTANOC synthesis

^{68}Ga-DOTANOC synthesis was carried out using the method previously detailed by Zhernosekov et al. [20] and is briefly described here: 30–50 mCi ^{68}Ge/^{68}Ga generator (Cyclotron Co Ltd., Obninsk, Russia) was eluted using 0.1 M hydrochloric acid (HCl). The eluent was loaded on a miniaturized column of organic cation-exchange resin to pre-concentrate and pre-purify (using 80 % acetone/0.15 M HCl). The processed ^{68}Ga was directly eluted with 97.7 % acetone/0.05 M HCl into the reaction vial containing 30–50 μg of DOTANOC. Synthesis was carried out at approximately 126 °C for 10–15 min. This was followed by removal of labeled peptide from unlabeled peptide using a reverse-phase C-18 column, using 400 μl of ethanol. This was further diluted with normal saline and passed through a 0.22-μm filter to obtain a sterile preparation for injection. A labeling yield of >95 % and specific activity (>15 GBq/μmol) were achieved after 10–15 min of heating.

^{68}Ga-DOTANOC PET/CT imaging

Fasting was not required. A dose of 132–222 MBq (4–6 mCi) of ^{68}Ga-DOTANOC was injected intravenously. After a 45- to 60-min uptake period PET/CT acquisition was started on a dedicated PET/CT scanner (Biograph 2, Siemens Medical Solutions, Erlangen, Germany). First, CT acquisition was performed on a spiral dual-slice CT with a slice thickness of 4 mm, pitch of 1, a matrix of 512×512 pixels, and pixel size of 1 mm. No oral or intravenous contrast was used in CT. After CT acquisition, 3-D PET acquisition of the same axial range was done from the base of the skull (including pituitary fossa) to mid thighs, using a matrix of 128×128 pixels and slice thickness of 1.5 mm. CT-based attenuation correction of the emission images was then applied. The PET images were reconstructed by iterative method ordered subset expectation maximization (OSEM) with two iterations and eight subsets. The reconstructed attenuation-corrected PET images, CT images, and fused images of matching pairs of PET and CT images were then available for review in axial, coronal, and sagittal planes, as well as in maximum intensity projections (MIP), 3-D cine mode.

^{131}I-MIBG imaging

In 40 patients ^{131}I-MIBG scintigraphy with/without SPECT/CT was done within ±2 weeks of PET/CT. None of the patients had received any drugs that would interfere with MIBG uptake, such as tricyclic antidepressants or sympathomimetic amines. Following the intravenous injection of a mean dose of 37±12 MBq of ^{131}I-MIBG (GE Healthcare, Braunschweig, Germany), a planar scintigraphy image was obtained with a large field of view dual-head gamma camera (Symbia E, Siemens Medical Solutions, Hoffman Estates, IL, USA) and a high energy-collimator. Whole-body images in the ventral and dorsal planes as well as target images of the abdomen were acquired 48 h after injection. In 20 patients, additional SPECT/CT of the adrenals was also performed. SPECT was done with the following parameters: 128×128 matrix, 120 projections in 3° angle increments, and an acquisition time of 40 s per projection. SPECT was followed by CT examination with acquisition parameters of 130 kV, 100 mAs, pitch of 1, and 512×512 matrix using standard filters. All SPECT/CT images were uniformly processed with commercially available e.soft software (Siemens Medical Solutions, Knoxville, TN, USA) on a Syngo nuclear medicine workstation (Siemens Medical Solutions, Hoffman Estates, IL, USA).

Image analysis

^{68}Ga-DOTANOC PET/CT studies were evaluated by two experienced nuclear medicine physicians. To provide a "clean" analysis of PET/CT results they were blinded to the patient's clinical, biochemical, and previous imaging findings. Their findings were concordant for 60 of the 62 patients. For the remaining two patients a consensus diagnosis was reached after discussion. For qualitative evaluation of PET/CT images the presence of an adrenal lesion (nodule/mass) on CT showing visual ^{68}Ga-DOTANOC uptake was taken as positive for pheochromocytoma. Care was taken not to confuse the physiological uptake in the adrenal gland for tumor uptake. In the absence of a definite adrenal lesion on PET/CT, asymmetrically increased ^{68}Ga-DOTANOC uptake in an adrenal was taken as positive. Any other nonphysiological focal area of increased ^{68}Ga-DOTANOC uptake was looked for and was classified as a second primary or metastasis. For the purpose of quantitative analysis the maximum standardized uptake values (SUV_{max}) and average SUV (SUV_{mean}) were measured for all adrenal lesions, normal liver, and the unaffected adrenal (if present). The SUV_{mean} and SUV_{max} were measured by drawing an isocontour to delineate 50 % of the highest radioactivity concentration as a 50 % cutoff region of interest (ROI). If a primary tumor was not found, the highest SUV in the adrenal glands was recorded. A large circular ROI was drawn in the posterior part of the right liver lobe, and the SUV_{mean} of the liver (SUV_{liver}) was

recorded. SUV_{max} was also recorded for the second primary or metastatic lesions, if present. All SUV calculation was done via the default method by body weight [SUV=mean ROI activity (MBq/g)/injected dose (MBq)/body weight (g)].

^{131}I-MIBG images were evaluated by two experienced nuclear medicine physicians independently, blinded to clinical, biochemical, and other imaging findings. Any focal accumulation of ^{131}I-MIBG in the adrenal glands or extra-adrenal regions that exceeded the normal regional tracer uptake was considered abnormal. They were in agreement for 37 of 40 patients. For the remaining three patients a consensus was reached after discussion.

Reference standard

Histopathology was used as reference standard for 52 lesions (48 pheochromocytomas, 3 adenomas, and 1 adrenocortical carcinoma). For the remaining 18 lesions, a combination of clinical, biochemical, and imaging follow-up of at least 6 months was used as reference standard (2 pheochromocytomas and 16 adenomas/normal adrenals) as tumor biopsy is contraindicated in these groups of neoplasms. The median duration of follow-up was 9 months (range 6–36 months). Based on these above-mentioned reference standards, 50/70 (71.4 %) lesions were proven to be pheochromocytoma. The diagnosis of malignant pheochromocytoma was considered if there was clear documentation of metastasis on histopathology and/or imaging. Medullary thyroid carcinoma (MTC) in all five patients (four thyroidal and one nodal) was histologically/cytologically confirmed.

Statistical analysis

All statistical analysis was done using MedCalc 11.3.0.0 (MedCalc Software, Acacialaan, Ostend, Belgium). The Kolmogorov-Smirnov test was used to check the normality of the data. The Wilcoxon rank sum test was used to compare paired data and Mann-Whitney U test for unpaired data. Spearman's correlation coefficient analysis was used to test the association of two variables. Receiver-operating characteristic curve (ROC) analysis was done to derive cutoff levels for SUV parameters. McNemar's test was used to compare the diagnostic accuracy of ^{68}Ga-DOTANOC PET/CT with ^{131}I-MIBG scintigraphy. A p value<0.05 was considered significant.

Results

Patient characteristics

Patient characteristics are detailed in Table 1. In 30 patients only one of the biochemical markers detailed in the "Materials

Table 1 Patient characteristics

Characteristics	Value
Age (years)	
Mean±SD	34.3±16.1
Range	9–72
Sex	
Male	38 (61.2 %)
Female	24 (38.7 %)
MEN syndrome	
Yes	14 (22.5 %)
MEN2A	12 (19.3 %)
MEN2B	02 (3.2 %)
No	48 (77.4 %)
Malignant pheochromocytoma	
Yes	07 (11.3 %)
No	55 (88.7 %)
Biochemical markers	
Elevated	54 (87 %)
Normal	06 (9.6 %)
CT findings[a]	
Mass (3 cm)	37 (52.8 %)
Nodule (<3 cm)	17 (24.2 %)
Asymmetry/thickening	16 (23 %)

MEN multiple endocrine neoplasia

[a] Of 70 suspicious adrenals

Table 2 Diagnostic accuracy of ^{68}Ga-DOTANOC PET/CT for pheochromocytoma on patient wise and lesion wise analysis (results with 95 % confidence interval)

Parameter	^{68}Ga-DOTANOC PET/CT	
	Patient wise ($n = 62$)	Lesion wise ($n = 70$)
Sensitivity	90.4 % (77.4–97.3)	92 % (80.7–97.8)
Specificity	85 % (62.1–96.8)	85 % (62.1–96.7)
PPV	92.7 % (80–98.5)	93.8 % (83.1–98.7)
NPV	81 % (58–94.5)	80.9 % (58–94.5)
Accuracy	88.7 %	90 %

PPV positive predictive value, *NPV* negative predictive value

and methods" section was elevated. In the remaining 32 patients, variable combination of these markers was elevated. As different biochemical markers were available for different patients, these are not detailed.

^{68}Ga-DOTANOC PET/CT diagnostic accuracy

Patient-based analysis

^{68}Ga-DOTANOC PET/CT was interpreted as positive for pheochromocytoma in 41/62 (66.1 %) and negative in 21/62 (33.9 %) patients. On a patient-based analysis it was true-positive (TP) in 38, true-negative (TN) in 17, false-positive (FP) in 3, and false-negative (FN) in 4 patients (Table 2).

Lesion-based analysis

Of the total 70 lesions seen on CT, ^{68}Ga-DOTANOC PET/CT was interpreted as positive for pheochromocytoma in 49/70 (70 %) and negative in 21/70 (30 %). On a lesion-based analysis it was TP in 46, TN in 17, FP in 3, and FN in 4 patients (Table 2). All three FP lesions on PET/CT were found to be adenoma at histopathology. In three of the four FN lesions, no mass/nodule was seen on the non-contrast CT part

of PET/CT. While one patient had a definite nodule (1.1 cm), the remaining three showed only asymmetrical thickening.

MEN2 syndrome

Among 14 patients with MEN2, ^{68}Ga-DOTANOC PET/CT was positive for pheochromocytoma in 9 and negative in 5. In these patients with 18 suspicious adrenal lesions on CT, PET/CT was TP for 13 and TN for 5 lesions. There were no FP or FN lesions (accuracy 100 %). In addition, ^{68}Ga-DOTANOC PET/CT also demonstrated MTC in four patients (two primary and two recurrent) and nodal metastasis from MTC in one patient.

Malignant pheochromocytoma

^{68}Ga-DOTANOC PET/CT was positive for pheochromocytoma in all seven patients with malignant pheochromocytoma (nine lesions, accuracy 100 %). In all these seven patients ^{68}Ga-DOTANOC PET/CT also demonstrated metastases. The metastatic sites were node in six patients, bone in three, liver in three, and lung in one. In three patients there was more than one site of metastasis. In one patient, ^{68}Ga-DOTANOC PET/CT also demonstrated a synchronous thoracic paraganglioma.

Semiquantitative analysis

Overall

The details of various SUV parameters are presented in Table 3. Size and all SUV parameters were significantly higher for pheochromocytoma than that for other adrenal lesions (Table 4 and Fig. 1). Unpaired and paired analyses were performed to compare the SUV parameters in tumors and normal adrenal glands. At unpaired analysis comparing tumors with all normal glands, the SUV_{max} but not SUV_{mean} of the adrenal tumors was significantly higher (Table 4). For paired analysis patients with bilateral tumors and unilateral

Table 3 Results of semiquantitative analysis of ^{68}Ga-DOTANOC PET/CT

Parameter	Mean±SD	Median	Range
Tumor SUV$_{max}$	10.1±9.7	6.7	0.4–44.4
Tumor SUV$_{mean}$	6.4±6.2	3.9	0.2–26.4
SUV$_{liver}$	2.1±1.6	1.7	0.2–7.8
Tumor SUV$_{max}$/SUV$_{liver}$	5±3.1	4.7	0.5–15
Tumor SUV$_{mean}$/SUV$_{liver}$	3.2±2	3.1	0.4–10.3
Normal adrenal SUV$_{max}$	6.7±6.3	4.1	0.3–30.4
Normal adrenal SUV$_{mean}$	4.8±4.6	2.9	0.2–20.7
Metastasis SUV$_{max}$	5.7±4.2	5.1	0.7–16

adrenals were excluded, and tumor SUV parameters were compared with contralateral normal adrenal. On paired analysis both SUV$_{max}$ and SUV$_{mean}$ of adrenal tumors was significantly higher (Table 4). On ROC analysis (Table 5) a significant cutoff could be derived for all SUV parameters. Among these parameters, a tumor SUV$_{max}$/SUV$_{liver}$ cutoff of >2.5 showed the highest diagnostic accuracy (AUC 0.741, 95 % confidence interval 0.622–0.838).

MEN2 syndrome

Comparison of size and SUV parameters of the tumors among patients with and without MEN2 is detailed in Table 4. While the SUV$_{max}$ and SUV$_{mean}$ of tumors were significantly higher in patients with MEN2, no difference was noted for other parameters.

Malignant pheochromocytoma

The comparison of size and SUV parameters of the tumors among patients with benign and malignant

pheochromocytoma is detailed in Table 4. No significant difference was found between benign and malignant pheochromocytoma for any of these parameters.

Correlation with tumor size

The mean tumor size was 4.1±2.4 cm (median 3.8, range 0.6–11). We assessed the relationship between lesion size and the respective SUV parameters to see whether tumor size correlated with SSTR expression. No significant correlation was noted between tumor size and tumor SUV$_{max}$ ($\rho=0.227$, $p=0.099$), tumor SUV$_{mean}$ ($\rho=0.155$, $p=0.262$), tumor SUV$_{max}$/SUV$_{liver}$ ($\rho=0.131$, $p=0.347$), and tumor SUV$_{mean}$/SUV$_{liver}$ ($\rho=0.092$, $p=0.510$).

Comparison with ^{131}I-MIBG imaging

Overall

Both ^{68}Ga-DOTANOC PET/CT and ^{131}I-MIBG imaging were available for 45 adrenal lesions in 40 patients (Figs. 2–5). The sensitivity, specificity, positive predictive value (PPV), negative predictive value (NPV), and accuracy of both imaging methods for these 45 lesions are detailed in Table 6. On a lesion-based comparison ^{68}Ga-DOTANOC PET/CT was superior to ^{131}I-MIBG imaging for pheochromocytoma ($p=0.035$). Results of ^{68}Ga-DOTANOC PET/CT and ^{131}I-MIBG imaging were discordant for 15/45 (33.3 %) lesions.

MEN2 syndrome

In patients with MEN2, both ^{68}Ga-DOTANOC PET/CT and ^{131}I-MIBG were available for 14/18 adrenal lesions. ^{68}Ga-DOTANOC PET/CT was TP in ten and TN in four, while

Table 4 Comparison of size and SUV parameters between subgroups

Parameter	Mean±SD				
	Tumor size (cm)	Tumor SUV$_{max}$	Tumor SUV$_{mean}$	Tumor SUV$_{max}$/SUV$_{liver}$	Tumor SUV$_{max}$/SUV$_{liver}$
Pheochromocytoma vs other lesions[a]	4.4±2.4 vs 2.3±1.4 $p=0.030$	11.9±10.7 vs 5.5±4 $p=0.005$	7.5±6.8 vs 3.7±2.9 $p=0.022$	5.7±3.1 vs 3.2±2.5 $p=0.001$	3.5±2 vs 2.2±1.9 $p=0.003$
MEN2 vs sporadic tumors	3.8±2.5 vs 4.3±2.4 $p=0.395$	17±14.3 vs 7.7±6 $p=0.012$	10.5±8.6 vs 5±4.4 $p=0.011$	5.5±3 vs 4.8±3.2 $p=0.316$	3.4±1.9 vs 3±2.1 $p=0.367$
Benign vs malignant pheochromocytoma	3.9±2.4 vs 5.5±2.2 $p=0.073$	9.3±8.4 vs 15.3±15.6 $p=0.269$	6±5.4 vs 9.2±10 $p=0.533$	4.9±3.3 vs 5.5±2.1 $p=0.380$	3.2±2.2 vs 3±1.1 $p=0.909$
Tumor vs unpaired adrenal	–	10.1±9.7 vs 6.7±6.3 $p=0.026$	6.4±6.2 vs 4.8±4.6 $p=0.137$	–	–
Tumor vs paired adrenal	–	10.1±9.7 vs 6.4±6 $p=0.002$	6.4±6.2 vs 4.6±4.3 $p=0.012$	–	–

[a] Based on reference standard

Fig. 1 Box and whisker plots comparing the SUV parameters between non-pheochromocytoma adrenal lesions (*solid boxes*) and pheochromocytoma (*dashed boxes*). The *circles* represent the outliers
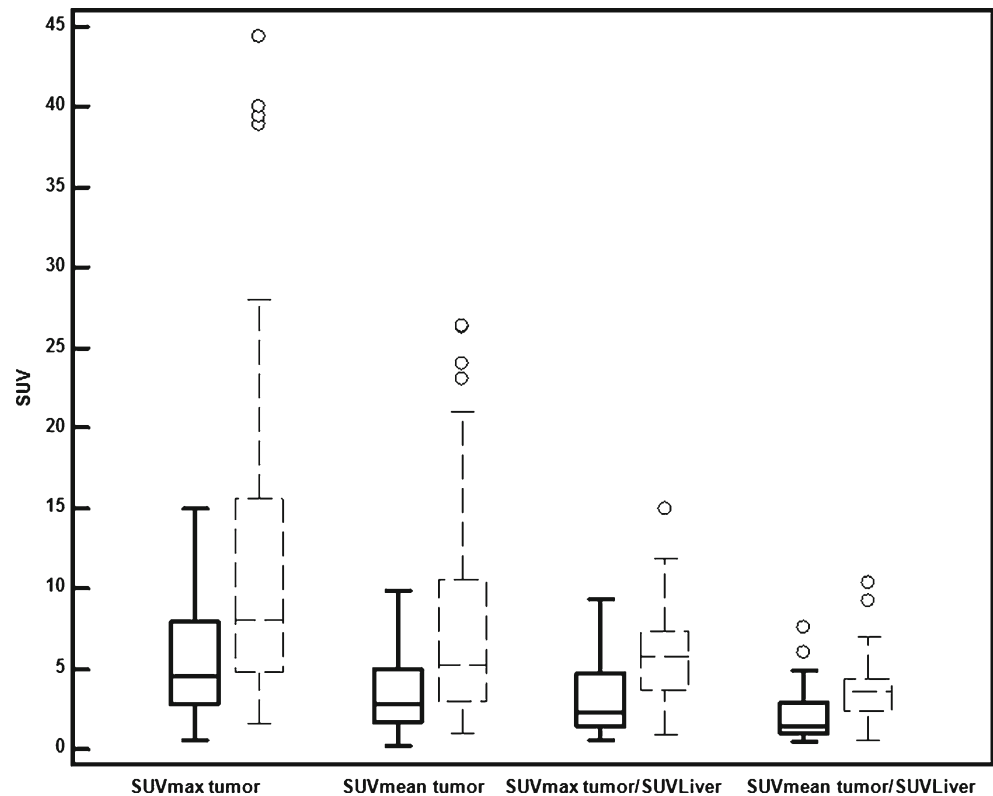
^{131}I-MIBG was TP in eight, TN in four, and FN in two. On lesion-based analysis no significant difference was seen between ^{68}Ga-DOTANOC PET/CT and ^{131}I-MIBG ($p = 0.500$). ^{131}I-MIBG imaging demonstrated MTC in only one of four patients with MEN syndrome and failed to show neck node metastasis from MTC in one patient. All these MTC lesions were positive on ^{68}Ga-DOTANOC PET/CT.

Malignant pheochromocytoma

Comparable ^{68}Ga-DOTANOC PET/CT and ^{131}I-MIBG images were available for five of seven patients (five adrenal lesions) with malignant pheochromocytoma. While ^{68}Ga-DOTANOC PET/CT was positive for pheochromocytoma in all, ^{131}I-MIBG was positive in three of five (60 %). In addition, ^{131}I-MIBG imaging failed to show metastatic disease in three of five patients (60 %) with malignant

Table 5 Results of ROC analysis

Parameters	Cutoff	Sensitivity	Specificity	AUC	p value
Tumor SUV_{max}	5.4	70 %	70 %	0.712	0.0009
Tumor SUV_{mean}	2.4	80 %	50 %	0.695	0.009
Tumor SUV_{max}/ SUV_{liver}	2.5	86 %	60 %	0.741	0.0001
Tumor SUV_{mean}/ SUV_{liver}	2.53	72 %	75 %	0.727	0.0003

pheochromocytoma, all of which were picked up by ^{68}Ga-DOTANOC PET/CT.

Discussion

Pheochromocytomas routinely express SSTRs, predominantly SSTR3 and to some extent SSTR2 [14]. This forms the basis of SSTR-based SPECT and PET imaging in pheochromocytoma. Results of ^{111}In-octreotide SPECT imaging in pheochromocytoma have generally been poor and inferior to MIBG imaging, with better results reported for malignant than benign pheochromocytoma [21]. Apart from the issue of limited resolution, this might have also been because of predominant affinity of ^{111}In-octreotide towards SSTR2, rather than SSTR3 [22]. More recently SSTR-based PET/CT imaging of pheochromocytoma has been attempted using ^{68}Ga-DOTA-peptides with encouraging results [15–19]. PET/CT imaging with these agents has already been shown to be superior to ^{111}In-octreotide SPECT [23], though data pertaining specifically to pheochromocytoma are lacking. Among the ^{68}Ga-DOTA-peptides, ^{68}Ga-DOTANOC appears to be of particular interest because of its broader SSTR affinity, including intermediate to low affinity for SSTR3 [24, 25], the predominant subtype in most pheochromocytomas [14]. Surprisingly, most of the previous studies have employed ^{68}Ga-DOTATOC [17] or ^{68}Ga-DOTATATE [15, 16, 19] for imaging of pheochromocytoma,
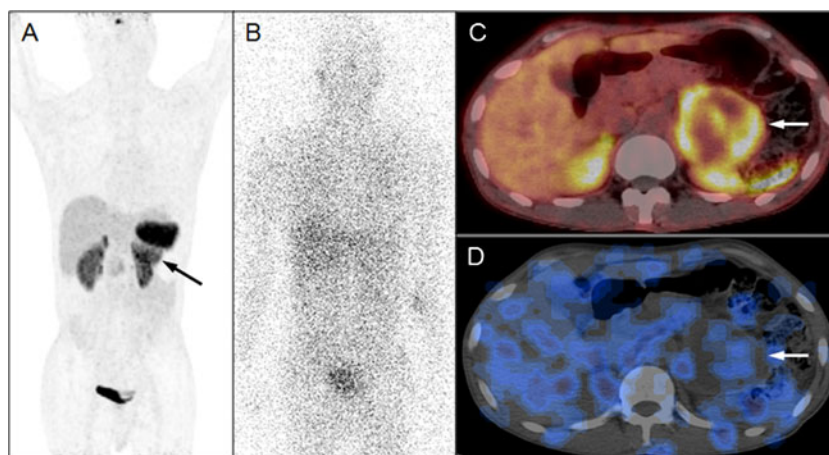
Fig. 2 A 37-year-old man with headache, paroxysmal hypertension, elevated 24-h urinary metanephrine, and left adrenal mass on CT. MIP ^{68}Ga-DOTANOC PET image (**a**) shows abnormal radiotracer uptake in the left suprarenal region (*arrow*), corresponding to the necrotic left adrenal mass on PET/CT image (**c**, *arrow*). Anterior ^{131}I-MIBG scintigraphy image (**b**) is normal and on SPECT/CT image no ^{131}I-MIBG uptake is seen in the adrenal mass (*arrow*). The patient underwent surgery and the diagnosis of pheochromocytoma was confirmed

both of which have no significant affinity for SSTR3. Moreover, these studies suffered from the drawbacks of small sample sizes and mixed patient populations. To address these limitations, the present study assessed the diagnostic accuracy of ^{68}Ga-DOTANOC PET/CT in a large population of patients with suspected pheochromocytoma. The present study differs from the pilot study conducted at our center by Naswa et al. [18] in certain important aspects. First is the larger sample

size. Second, the present study evaluated an exclusive population of pheochromocytoma, while that by Naswa et al. [18] evaluated a mixed population of pheochromocytoma and paraganglioma. Third, we have also done in-depth analysis of SUV parameters, which was not attempted in the pilot study.

In the present study, ^{68}Ga-DOTAOC PET/CT showed high diagnostic accuracy on both patient-based and lesion-based analysis (88.7 and 90 %, respectively). It was FP only for three adrenal lesions (size <1.5 cm), all of which turned out to be benign adenoma at histopathology. Two factors probably accounted for the FP results. First, since high ^{68}Ga-DOTANOC uptake is seen in normal adrenals [26], differentiation of tumor uptake from tracer uptake in normal adrenal medulla is sometimes difficult, especially if the adrenal lesion is small. Second, some of the cortical adenomas can also demonstrate low-grade SSTR expression [27], resulting in FP findings. Because we did not have the SSTR profile of the resected specimens, we were not able to confirm these hypotheses in the present study. ^{68}Ga-DOTANOC PET/CT was FN for three lesions. Definite adrenal nodule on CT was seen in only one of these four lesions, with the remaining three showing asymmetrical thickening. In fact, ^{68}Ga-DOTANOC PET/CT was interpreted as negative for all 16 lesions without adrenal nodule/mass on CT. This is because of the limitation that it is not always possible to differentiate physiological from pathological uptake at visual PET analysis alone if CT does not show a definite mass or nodule. Therefore, ^{68}Ga-DOTANOC PET/CT seems to be most useful when there is a definite adrenal mass or nodule at CT in the clinical setting of pheochromocytoma. The values of diagnostic accuracy reported in this study are lower than those of Naswa et al. [18]. The main reason for this difference is probably the preponderance of paraganglioma in their study population. On ^{68}Ga-DOTANOC PET/CT, evaluation and
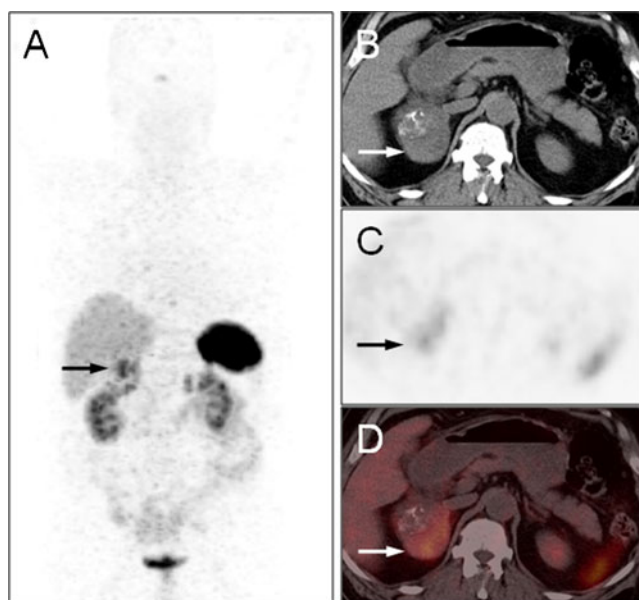

Fig. 3 A 67-year-old man with uncontrolled hypertension and right adrenal mass on CT. The 24-h urinary metanephrines were elevated. MIP ^{68}Ga-DOTANOC PET (**a**) image showed mildly increased abnormal tracer uptake in the right suprarenal region (*arrow*). Axial non-contrast CT (**b**) image of the abdomen shows a right adrenal mass (*arrow*) with areas of calcification and cystic degeneration. The mass shows mild ^{68}Ga-DOTANOC uptake (SUV$_{max}$ 1.6) on PET (**c**) and PET/CT (**d**) images (*arrow*). The patient underwent surgery and postoperative histopathology confirmed the diagnosis of pheochromocytoma

Fig. 4 A 56-year-old man with left adrenal incidentaloma on CT and elevated plasma norepinephrine. MIP ^{68}Ga-DOTANOC PET image (**a**) and anterior ^{131}I-MIBG scintigraphy image (**b**) are normal. On PET/CT image the left adrenal mass (**c**, *arrow*) does not show any significant ^{68}Ga-DOTANOC uptake. Similarly, on SPECT/CT image no ^{131}I-MIBG uptake is seen in the left adrenal mass (**d**, *arrow*). Postoperative histology revealed pheochromocytoma
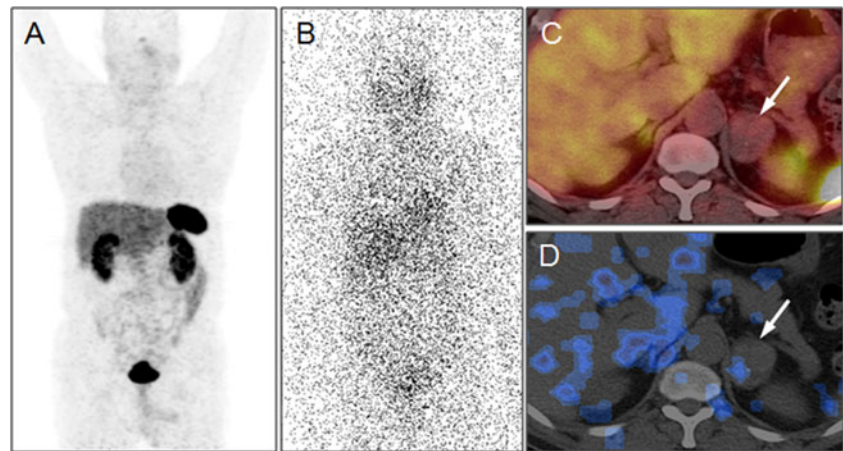
identification of lesions at extra-adrenal sites is easier due to the lack of physiological tracer uptake. In addition, it is known that paragangliomas show higher levels of SSTR expression than pheochromocytomas. At semiquantitative analysis, wide variation was seen in SUV parameters for the tumors as well as normal adrenals. However, a major inference that could be derived is that pheochromocytomas have higher SUV parameters than other adrenal lesions, reconfirming high in vivo SSTR expression. Although there was significant difference between the SUV_{max} of tumors with paired and unpaired normal adrenal glands ($p = 0.002$ and 0.026, respectively), considerable overlap was seen between these values. Using ROC analysis we were able to find significant cutoffs for all SUV parameters for differentiating pheochromocytoma from other adrenal lesions. Among these, tumor SUV_{max}/SUV_{liver} showed the highest diagnostic accuracy. However, the sensitivity and specificity of these SUV parameter cutoffs is only modest and inferior to visual

analysis. Hence, the proposed thresholds might not be suitable for routine application in clinical practice.

In patients with MEN2 ^{68}Ga-DOTANOC PET/CT showed excellent results for detection of pheochromocytoma. There were no FP or FN results, thus showing the utility of ^{68}Ga-DOTANOC PET/CT in MEN2 with suspected pheochromocytoma. However, all these patients had clinical/biochemical suspicion along with suspicious adrenal lesions at CT. Hence, whether the same success can be replicated in screening of asymptomatic cases with MEN2 needs to be established. ^{68}Ga-DOTANOC PET/CT also detected associated MTC in five patients, for which it has known utility [28]. The SUV_{max} and SUV_{mean} of the adrenal tumors in patients with MEN2 were significantly higher than sporadic tumors. Although the exact cause of this finding is unclear, this finding has also been previously reported in a rat model [29]. ^{68}Ga-DOTANOC PET/CT also showed excellent results in patients with malignant pheochromocytoma. Primary
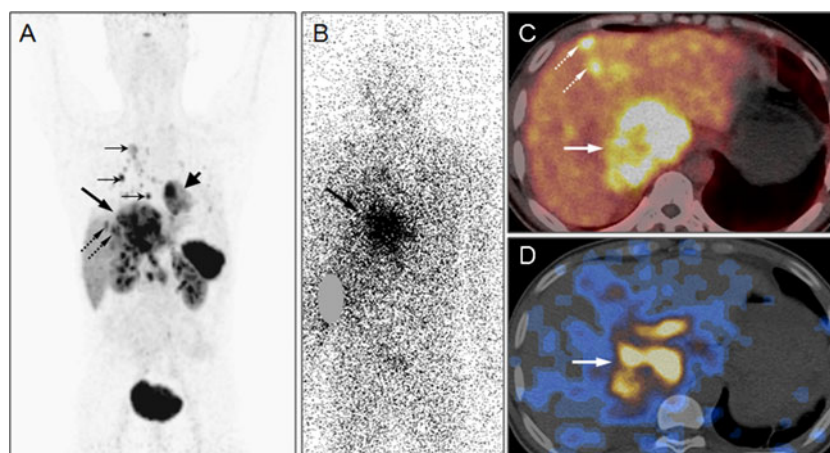

Fig. 5 A 27-year-old man with headache, palpitations, and uncontrolled hypertension, along with right adrenal mass and multiple hepatic lesions on CT. MIP PET image (**a**) shows ^{68}Ga-DOTANOC uptake in right adrenal mass (*bold arrow*), with multiple liver metastases (*broken arrows*), mediastinal paraganglioma (*arrowhead*), and pulmonary metastases (*arrows*). Axial PET/CT image (**c**) shows ^{68}Ga-DOTANOC avid right adrenal mass (*bold arrow*) and liver metastases (*broken arrows*). Anterior ^{131}I-MIBG scintigraphy image (**b**) shows only the left adrenal mass (*bold arrow*). On axial SPECT/CT image (**d**) only the ^{131}I-MIBG avid left adrenal mass is seen (*bold arrow*). Biopsy from the liver lesions confirmed metastatic pheochromocytoma and the patient is undergoing peptide receptor radionuclide therapy

Table 6 Comparative diagnostic accuracy of ^{68}Ga-DOTANOC PET/CT and ^{131}I-MIBG imaging on lesion wise analysis (results with 95 % confidence interval)

Parameter	^{68}Ga-DOTANOC PET/CT	^{131}I-MIBG imaging
Sensitivity	93.5 % (78.5–99.2)	61.2 % (42.1–78.1)
Specificity	85.7 % (57.1–98.2)	78.5 % (49.2–95.3)
PPV	93.5 % (78.5–99.2)	86.3 % (65–97)
NPV	85.7 % (57.1–98.2)	47.8 % (26.8–69.4)
Accuracy	91.1 %	66.6 %

PPV positive predictive value, *NPV* negative predictive value

tumor as well as metastasis was identified in all seven patients. Similar results were also reported by Kroiss et al. [17] in their study in patients with metastatic pheochromocytoma and neuroblastoma. We found no significant difference between malignant and benign pheochromocytoma with respect to SUV parameters, probably reflecting overlap of SSTR expression.

On a lesion-based comparison, ^{68}Ga-DOTANOC PET/CT showed a significantly higher accuracy as compared to ^{131}I-MIBG (91.1 vs 66.6 %, $p = 0.035$). These findings are similar to those reported by Naswa et al. [18] and Maurice et al. [19]. However, in patients with MEN2, no significant difference was found between ^{68}Ga-DOTANOC PET/CT and ^{131}I-MIBG for adrenal lesions ($p = 0.500$). This equality is probably the result of high accuracy of MIBG imaging for detection of pheochromocytoma in MEN2 [30] coupled with the small number of MEN2 patients in the present study. While further studies are required to make definitive comment, given the fact that ^{68}Ga-DOTANOC PET/CT is also useful for imaging MTC, it may be preferred over MIBG imaging in patients with MEN2. In patients with malignant pheochromocytoma ^{68}Ga-DOTANOC PET/CT showed primary tumor and metastasis in all patients, while ^{131}I-MIBG scintigraphy was negative for pheochromocytoma in two of five patients and metastasis in three of five patients. Given the small number of patients statistical comparison was not attempted. We would like to highlight that ^{131}I-MIBG, not ^{123}I-MIBG, was used in the present study. The latter allows a higher dose, gives a high photon flux, and provides better image quality. Unfortunately, ^{123}I-MIBG is not available in our country and cannot be imported because of the short half-life ($T_{1/2}$ 13 h) and high cost. One might argue that the use of ^{123}I-MIBG might have altered our results. However, the superiority of ^{123}I-MIBG over ^{131}I-MIBG in pheochromocytoma is only marginal [31]. In addition, the sensitivity of ^{131}I-MIBG for pheochromocytoma in the present study is similar to those reported for ^{123}I-MIBG by Kroiss et al. (61.2 and 63.3 %, respectively) [17]. Therefore, it is unlikely that use of ^{123}I-MIBG would have significantly altered the results. On the other hand, a recent study has demonstrated the superiority of ^{131}I-MIBG SPECT/CT over SPECT and planar imaging in pheochromocytoma [8]. Hence, the lack of SPECT/CT in all patients might have compromised the performance of ^{131}I-MIBG imaging in the present study.

Other PET tracers which can be employed for imaging of pheochromocytoma include ^{18}F-FDG to assess glucose metabolism, ^{11}C-HED and ^{18}F-FDA for catecholaminergic phenotype, and ^{18}F-FDOPA for assessing amine uptake and decarboxylation. The most commonly used PET tracer ^{18}F-FDG has shown low sensitivity but high specificity, comparable to ^{123}I-MIBG imaging in pheochromocytoma [9]. It is particularly useful in metastatic pheochromocytoma and might have played a complementary role to ^{68}Ga-DOTANOC PET/CT in the present population. ^{18}F-FDOPA PET/CT has demonstrated high sensitivity and specificity for pheochromocytoma [10]. Minimal uptake of ^{18}F-FDOPA in normal adrenal glands is advantageous when interpreting PET/CT images for pheochromocytoma. ^{18}F-FDA PET/CT also has demonstrated encouraging results in pheochromocytoma and it is superior to both ^{18}F-FDOPA PET/CT and ^{123}I-MIBG for metastatic lesions [11]. ^{11}C-HED is another PET/CT tracer showing high accuracy for pheochromocytoma [12]. Given the high diagnostic accuracy shown by ^{68}Ga-DOTANOC PET/CT in the present study, a head to head comparison with these other PET tracers is warranted to find the optimum agent for different subgroups of pheochromocytoma. The points in favor of ^{68}Ga-DOTANOC are its easy generator-based synthesis as compared to difficult synthesis (^{18}F-FDOPA, ^{18}F-FDA) or need for on-site cyclotron (^{11}C-HED) for other tracers. Additionally, ^{68}Ga-DOTANOC PET/CT can help in selection of patients (inoperable/metastatic) for peptide receptor radionuclide therapy, which is currently not possible with other PET tracers.

A few limitations of the present study must be acknowledged. First is the retrospective design. Second, histopathological diagnosis was not available for all the adrenal lesions. Although this would have been ideal, it was not ethically feasible. Hence, we employed a combination of clinical, biochemical, and imaging follow-up of at least 6 months to confirm or rule out pheochromocytoma, which is an accepted method. Third, ^{131}I-MIBG SPECT/CT images were not available for all patients, as at our center, like most others, the decision to perform SPECT/CT is guided by planar imaging. Finally, the lack of knowledge regarding the succinate dehydrogenase (SDH) status, which is pivotal to understanding the results of functional imaging of pheochromocytomas, was a major limitation of the present study. Germline mutations in SDH enzyme gene (especially subunit B) occur in a subset of patients with pheochromocytoma. SDH status appears to be a critical parameter determining the prognosis as well as selecting the best functional imaging agent for pheochromocytomas and

paragangliomas [32, 33]. Future prospective studies addressing these shortcomings and comparing ^{68}Ga-DOTANOC with other PET tracers are warranted.

Conclusion

^{68}Ga-DOTANOC PET/CT demonstrates high diagnostic accuracy in patients with clinical/biochemical suspicion of pheochromocytoma and adrenal abnormality at contrast CT and is superior to ^{131}I-MIBG imaging for this purpose. Best results of ^{68}Ga-DOTANOC PET/CT are seen in patients with MEN2-associated and malignant pheochromocytoma.

Conflicts of interest   None.

References

1. Werbel SS, Ober KP. Pheochromocytoma. Update on diagnosis, localization, and management. Med Clin North Am 1995;79:131–53.
2. Manger WM, Gifford RW. Pheochromocytoma: a clinical overview. In: Laragh JH, Brenner BM, editors. Hypertension: pathophysiology, diagnosis and management. New York: Raven; 1995. p. 225–44.
3. Neumann HPH, Berger DP, Sigmund G, Blum U, Schmidt D, Parmer RJ, et al. Pheochromocytomas, multiple endocrine neoplasia type 2, and von Hippel-Lindau disease. N Engl J Med 1993;329:1531–8.
4. Lenders JW, Pacak K, Walther MM, Linehan WM, Mannelli M, Friberg P, et al. Biochemical diagnosis of pheochromocytoma: which test is best? JAMA 2002;287:1427–34.
5. Quint LE, Glazer GM, Francis IR, Shapiro B, Chenevert TL. Pheochromocytoma and paraganglioma: comparison of MR imaging with CT and I-131 MIBG scintigraphy. Radiology 1987;165:89–93.
6. Bombardieri E, Giammarile F, Aktolun C, Baum RP, Bischof Delaloye A, Maffioli L, et al. 131I/123I-metaiodobenzylguanidine (mIBG) scintigraphy: procedure guidelines for tumour imaging. Eur J Nucl Med Mol Imaging 2010;37:2436–46.
7. Feggi L, Degli Uberti E, Pansini GC, Transforini G, Prandini N, Ambrosio MR, et al. Pitfalls in scintigraphic detection of neuroendocrine tumours. Eur J Nucl Med 1992;19:214–8.
8. Sharma P, Dhull VS, Jeph S, Reddy RM, Singh H, Naswa N, et al. Can hybrid SPECT-CT overcome the limitations associated with poor imaging properties of 131I-MIBG?: comparison with planar scintigraphy and SPECT in pheochromocytoma. Clin Nucl Med 2013;38:e346–53.
9. Timmers HJ, Chen CC, Carrasquillo JA, Whatley M, Ling A, Eisenhofer G, et al. Staging and functional characterization of pheochromocytoma and paraganglioma by 18F-fluorodeoxyglucose (18F-FDG) positron emission tomography. J Natl Cancer Inst 2012;104:700–8.
10. Fiebrich HB, Brouwers AH, Kerstens MN, Pijl ME, Kema IP, de Jong JR, et al. 6-[F-18]Fluoro-L-dihydroxyphenylalanine positron emission tomography is superior to conventional imaging with (123)I-metaiodobenzylguanidine scintigraphy, computer tomography, and magnetic resonance imaging in localizing tumors causing catecholamine excess. J Clin Endocrinol Metab 2009;94:3922–30.
11. Ilias I, Yu J, Carrasquillo JA, Chen CC, Eisenhofer G, Whatley M, et al. Superiority of 6-[18F]-fluorodopamine positron emission tomography versus [131I]-metaiodobenzylguanidine scintigraphy in the localization of metastatic pheochromocytoma. J Clin Endocrinol Metab 2003;88:4083–7.
12. Trampal C, Engler H, Juhlin C, Bergström M, Långström B. Pheochromocytomas: detection with 11C hydroxyephedrine PET. Radiology 2004;230:423–8.
13. Naji M, AL-Nahhas A. 68Ga-labelled peptides in the management of neuroectodermal tumours. Eur J Nucl Med Mol Imaging 2012;39:S61–7.
14. Mundschenk J, Unger N, Schulz S, Höllt V, Schulz S, Steinke R, et al. Somatostatin receptor subtypes in human pheochromocytoma: subcellular expression pattern and functional relevance for octreotide scintigraphy. J Clin Endocrinol Metab 2003;88:5150–7.
15. Win Z, Al-Nahhas A, Towey D, Todd JF, Rubello D, Lewington V, et al. 68Ga-DOTATATE PET in neuroectodermal tumours: first experience. Nucl Med Commun 2007;28:359–63.
16. Naji M, Zhao C, Welsh SJ, Meades R, Win Z, Ferrarese A, et al. 68Ga-DOTA-TATE PET vs. 123I-MIBG in identifying malignant neural crest tumours. Mol Imaging Biol 2011;13:769–75.
17. Kroiss A, Putzer D, Uprimny C, Decristoforo C, Gabriel M, Santner W, et al. Functional imaging in phaeochromocytoma and neuroblastoma with 68Ga-DOTA-Tyr 3-octreotide positron emission tomography and 123I-metaiodobenzylguanidine. Eur J Nucl Med Mol Imaging 2011;38:865–73.
18. Naswa N, Sharma P, Nazar AH, Agarwal KK, Kumar R, Ammini AC, et al. Prospective evaluation of 68Ga-DOTA-NOC PET-CT in phaeochromocytoma and paraganglioma: preliminary results from a single centre study. Eur Radiol 2012;22:710–9.
19. Maurice JB, Troke R, Win Z, Ramachandran R, Al-Nahhas A, Naji M, et al. A comparison of the performance of 68Ga-DOTATATE PET/CT and 123I-MIBG SPECT in the diagnosis and follow-up of phaeochromocytoma and paraganglioma. Eur J Nucl Med Mol Imaging 2012;39:1266–70.
20. Zhernosekov KP, Filosofov DV, Baum RP, Aschoff P, Bihl H, Razbash AA, et al. Processing of generator-produced 68Ga for medical application. J Nucl Med 2007;48:1741–8.
21. van der Harst E, de Herder WW, Bruining HA, Bonjer HJ, de Krijger RR, Lamberts SW, et al. [(123)I]metaiodobenzylguanidine and [(111)In]octreotide uptake in benign and malignant pheochromocytomas. J Clin Endocrinol Metab 2001;86:685–93.
22. Hofland LJ, Lamberts SW, van Hagen PM, Reubi JC, Schaeffer J, Waaijers M, et al. Crucial role for somatostatin receptor subtype 2 in determining the uptake of [111In-DTPA-D-Phe1]octreotide in somatostatin receptor-positive organs. J Nucl Med 2003;44:1315–21.
23. Srirajaskanthan R, Kayani I, Quigley AM, Soh J, Caplin ME, Bomanji J. The role of 68Ga-DOTATATE PET in patients with neuroendocrine tumors and negative or equivocal findings on 111In-DTPA-octreotide scintigraphy. J Nucl Med 2010;51:875–82.
24. Wild D, Mäcke HR, Waser B, Reubi JC, Ginj M, Rasch H, et al. 68Ga-DOTANOC: a first compound for PET imaging with high affinity for somatostatin receptor subtypes 2 and 5. Eur J Nucl Med Mol Imaging 2005;32:724.
25. Wild D, Schmitt JS, Ginj M, Mäcke HR, Bernard BF, Krenning E, et al. DOTA-NOC, a high-affinity ligand of somatostatin receptor subtypes 2, 3 and 5 for labelling with various radiometals. Eur J Nucl Med Mol Imaging 2003;30:1338–47.
26. Pettinato C, Sarnelli A, Di Donna M, Civollani S, Nanni C, Montini G, et al. 68Ga-DOTANOC: biodistribution and dosimetry in patients affected by neuroendocrine tumors. Eur J Nucl Med Mol Imaging 2008;35:72–9.
27. Unger N, Serdiuk I, Sheu SY, Walz MK, Schulz S, Saeger W, et al. Immunohistochemical localization of somatostatin receptor subtypes in benign and malignant adrenal tumours. Clin Endocrinol (Oxf) 2008;68:850–7.
28. Naswa N, Sharma P, Suman Kc S, Lata S, Kumar R, Malhotra A, et al. Prospective evaluation of 68Ga-DOTA-NOC PET-CT in patients with recurrent medullary thyroid carcinoma: comparison with 18F-FDG PET-CT. Nucl Med Commun 2012;33:766–74.
29. Miederer M, Molatore S, Marinoni I, Perren A, Spitzweg C, Reder S, et al. Functional imaging of pheochromocytoma with Ga-DOTATOC

and C-HED in a genetically defined rat model of multiple endocrine neoplasia. Int J Mol Imaging 2011;2011:175352.

30. Rodriguez JM, Balsalobre M, Ponce JL, Ríos A, Torregrosa NM, Tebar J, et al. Pheochromocytoma in MEN 2A syndrome. Study of 54 patients. World J Surg 2008;32:2520–6.

31. Furuta N, Kiyota H, Yoshigoe F, Hasegawa N, Ohishi Y. Diagnosis of pheochromocytoma using [123I]-compared with [131I]-metaiodobenzylguanidine scintigraphy. Int J Urol 1999;6:119–24.

32. Timmers HJ, Kozupa A, Eisenhofer G, Raygada M, Adams KT, Solis D, et al. Clinical presentations, biochemical phenotypes, and genotype-phenotype correlations in patients with succinate dehydrogenase subunit B-associated pheochromocytomas and paragangliomas. J Clin Endocrinol Metab 2007;92:779–86.

33. Havekes B, King K, Lai EW, Romijn JA, Corssmit EP, Pacak K. New imaging approaches to phaeochromocytomas and paragangliomas. Clin Endocrinol (Oxf) 2010;72:137–45.